Unraveling the structure of the h-BN/Rh(111) nanomesh with *ab initio* calculations

2008 J. Phys.: Condens. Matter 20 064207

(http://iopscience.iop.org/0953-8984/20/6/064207)

J. Phys.: Condens. Matter **20** (2008) 064207 (6pp) doi:10.1088/0953-8984/20/6/064207

Unraveling the structure of the h-BN/Rh(111) nanomesh with *ab initio* calculations

R Laskowski and P Blaha

Institute of Materials Chemistry, Vienna University of Technology, A-1060 Vienna, Austria

E-mail: rolask@theochem.tuwien.ac.at

Received 21 August 2007, in final form 6 September 2007
Published 24 January 2008
Online at stacks.iop.org/JPhysCM/20/064207

Abstract

The properties of a single layer of h-BN on top of a Rh(111) surface are discussed in terms of an *ab initio* generated force field approach as well as by direct *ab initio* density-functional theory (DFT) calculations. A single-layer model for the h-BN/Rh(111) nanomesh, in contrast to a previously considered (incomplete) double-layer model of h-BN, can explain the experimental data. The main focus of this work is to compare a force field approach described earlier in (Laskowski *et al* 2007 *Phys. Rev. Lett.* **98** 106802) with direct *ab initio* calculations. The calculated geometry of the h-BN layer is very similar to the structure predicted by the force field approach. The *ab initio* calculated density of states projected on N-$p_{x,y}$ of BN corresponding to 'low' and 'high' regions with respect to the Rh surface shows a 1 eV splitting and thus explains the observed σ-band splitting. Moreover, we find good agreement between calculated and experimental scanning tunneling microscope (STM) images of this system.

(Some figures in this article are in colour only in the electronic version)

1. Introduction

Self-assembling nanostructured materials are currently attracting great attention due to possible practical applications. Both theoretical and experimental approaches need to be combined in order to understand the complicated processes that lie behind the formation and functionality of these materials. In this paper we present an example where a theoretical approach based on *ab initio* calculations introduces a completely new interpretation of existing experimental results. It triggered new experiments, which in fact support the new structural model suggested by theory.

Recently, a self-assembling structure was detected when borazine is thermally decomposed on a Rh(111) surface [5]. Boron nitride forms a highly regular hexagonal nanostructure h-BN/Rh(111) with a periodicity of about 3.2 nm. The hexagonal unit cell consisting of a 12 × 12 Rh substrate, on which a 13 × 13 h-BN superstructure forms, was deduced from low-energy electron diffraction (LEED) patterns, surface x-ray diffraction [4], and STM pictures. A periodic hole structure with a diameter of about 2 nm was observed within this unit cell. Based on the STM images and on ultraviolet photoelectron spectroscopy (UPS) data, which showed a splitting of the BN-σ bands [5], an atomic model was suggested which consists of two incomplete boron nitride layers. The functionality of this nanomesh was demonstrated by decoration with C_{60} molecules [5]. Recently, an almost identical structure has been found on the Ru(0001) surface [7], whereas on Pd(111) [11], Pd(110) [6], and Pt(111) some kind of moiré pattern appears but on Ni(111) [12, 13, 1, 16, 8, 9] and Cu(111) [17] a simple epitaxial 1 × 1 h-BN monolayer forms. The initially proposed 'two-layer model' of the h-BN/Rh(111) nanomesh [5] is rather unrealistic due to many broken B–N bonds that occur in the incomplete h-BN layers. Our test calculations have shown that the resulting dangling bonds cause a high-energy penalty, making such structures highly unstable. Very recently, on the basis of an *ab initio* calculated force field approach, a new structure of this nanomesh has been proposed [10]. This structure consists of only a single layer of h-BN, which, however, is highly corrugated. The theoretically predicted corrugation is consistent with both the observed splitting of the BN-σ bands as well as with the experimental STM images. The model provides an understanding of the h-BN interaction with Rh surfaces, but extends to a wider class of systems like BN/Ru(001), BN/Pt(111) or even C/Ir(111) [14]. At the same time these complicated nanostructures can be

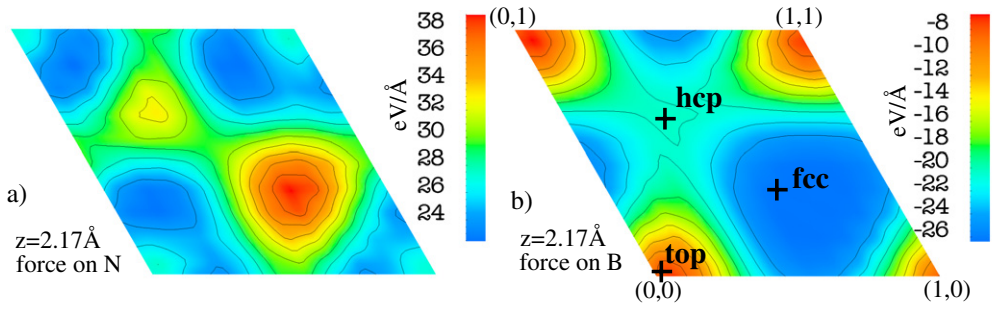

Figure 1. Surface map of the z force component acting on N and B atoms. The calculations are performed with a flat BN layer placed 2.17 Å from the surface. N is positioned at (x, y, z); B is at $(x + 2/3, y + 1/3, z)$.

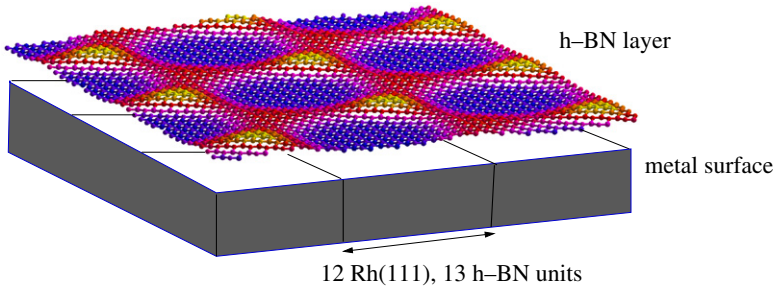

Figure 2. Schematic image of the corrugated h-BN layer on top of the Rh(111) surface. The periodicity of the layer is equal to 13 h-BN units and 12 Rh(111) units.

related to the simple 1 × 1 h-BN monolayers on Cu(111) and Ni(111). The theoretically proposed nanomesh model triggered new experiments [2] and in new STM images, where the long-range 3.2 nm periodicity has been 'filtered out', a continuous h-BN layer showed up, which fully supports the new structural model. Moreover, the conductivity maps scanned with bias voltages equal to the position of the split BN-σ bands clearly showed that the splitting originates from an alternating probing of 'low' and 'high' regions of the h-BN layer, which was one of the main results of [10].

The single-layer model of h-BN/Rh(111) [10] has been built on the basis of a force field approach. However, all components of the interaction field, which are crucial to the physics of the system, have been calculated *ab initio*. Nevertheless there were some essential approximations which had to be introduced into such model calculations, which can only be checked by full *ab initio* calculations. Here we report the results of such calculations performed within the DFT framework as implemented in the Wien2k [3] package. To our knowledge this is the first report of calculations for such a huge metallic system (consisting of 1108 atoms in the unit cell) with such a highly precise method.

2. Single-layer model of h-BN/Rh(111)

2.1. Ab initio force field approach

In order to keep the presentation self-contained we briefly repeat already published [10] results concerning the force field approach. We have observed that the interaction of a single h-BN layer with the metal surface strongly depends on the lateral x, y-position of the BN atoms relative to the Rh surface atoms. The force maps calculated in 1 × 1 geometry, where the h-BN bond length is stretched such that the unit cells of both h-BN and the underlying metal match, are presented in figure 1. (For computational details, see [10].) It is evident that, for a certain distance z above the Rh surface (close to the equilibrium BN-Rh distance), the B and N atoms are attracted (negative force) and repelled (positive force) from the surface, respectively. However the strength of this interaction depends on the x, y-position of BN. Note that the surface Rh atoms sit at the origin of the cell (top), while the sub- and subsub-surface atoms occupy the hexagonal close packed (hcp) and face-centered cubic (fcc) sites, respectively. When N sits on top of Rh and B therefore on fcc—called (fcc, top) BN—the repelling force on N is small while B is maximally attracted and thus BN is in a very stable position. On the other hand, BN at (hcp, top) or (fcc, hcp) would be in quite unfavorable positions, since the N repulsion dominates the B attraction.

Due to the strong elastic anisotropy (h-BN is rather stiff in the hexagonal plane but relatively flexible perpendicular to the plane), h-BN keeps its bond lengths rather unaffected when it covers the metal surface. Due to the lattice mismatch of about 7% between BN and Rh(111), the positions of the B and N atoms change periodically relative to the underlying metal surface, with a period of 12 Rh(111) or 13 h-BN lattice constants (this ratio gives an almost ideal 7% lattice mismatch). This lateral lattice mismatch leads to a deformation in the perpendicular direction, reflecting the shape and strength of the BN–metal interactions. The corrugation of h-BN is further controlled by the elastic constants describing the response of h-BN to the perpendicular deformations. A schematic presentation of the corrugated h-BN layer is shown on figure 2.

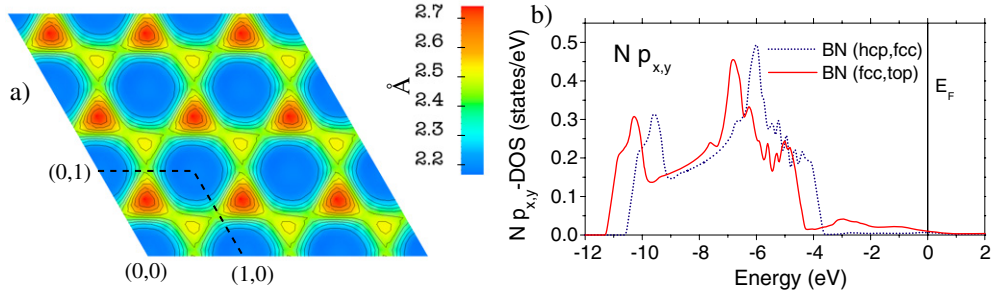

Figure 3. (a) Contour map of the z coordinate of N atoms in the 3 × 3 nanomesh unit cell predicted by the force field approach (measured from the top metal layer). (b) σ-band splitting (N-$p_{x,y}$ projected DOS calculated for low and high regions).

We have verified that the stretching of BN by 7% does not affect the values of the forces acting on the B and N atoms strongly. For that purpose, we performed a set of calculations in a 3 × 3 super-cell of h-BN/Rh(111), where part of the h-BN layer is relaxed such that it obtains the correct B–N bond length. No significant changes in the vertical BN forces were observed. Therefore force maps (presented above) calculated with 1 × 1 h-BN/Rh(111) geometry can be used directly to describe the interactions in the nanomesh unit cell. In order to obtain a complete force field, the h-BN positions above the 1 × 1-Rh(111) unit cell were sampled on a 10 × 10 × 8 mesh (440 separate self-consistent calculations). Additionally, the elastic response of the h-BN layer has been described by a force constant model, where deformations perpendicular and parallel to the hexagonal layer are included. All parameters have been calculated *ab initio*; for details, see [10].

Using the interactions described above, we have performed a structural optimization of the initially flat h-BN layer. The layer consists of a 13×13 h-BN supercell positioned on top of a 12 × 12 Rh(111) supercell. The metal interface layer has been kept frozen. The resulting N-z coordinates are displayed in figure 3(a). The BN layer is apparently strongly corrugated and the distance between N and the metal surface varies from 2.17 to 2.72 Å. One can clearly distinguish two regions. First, a rather flat area where BN is close to the metal, located around the origin of the unit cell, i.e. a region where the B and N atoms are close to their optimal (fcc, top) positions with respect to the underlying Rh atoms. We will call this the 'low' region, which covers about 70% of the nanomesh unit cell. When the B and N atoms cannot keep their optimal positions above Rh due to the lattice mismatch, they are repelled from the surface and a second region builds up, where BN is placed further away from the metal surface (the 'high' region). Within this 'high' region we can distinguish two slightly different heights of BN: a higher one and a lower one. The difference between these regions is that, around (1/3, 2/3), the B and N atoms are located close to (hcp, fcc) positions, whereas near (2/3, 1/3) they occupy (top, hcp) sites. The difference in height can be understood by inspecting the presented force maps (figure 1), where BN on (hcp, fcc) has the weakest attraction and strongest repulsion, respectively. The difference in the distance from the metal surface between the lowest and highest N atoms is close to 0.55 Å. The shape of the BN layer obviously reflects the measured STM images [5, 7].

The single-layer model of the h-BN nanomesh also explains the origin of the σ-band splitting (about 1 eV) observed in UPS measurements [5]. According to Corso *et al* [5], the splitting indicates the presence of two types of h-BN units and was the main justification for the proposed double-layer model. According to our model, however, the splitting is a result of simultaneous probing regions where the h-BN layer is close to or further away from the metal surface. These two regions contribute to either the lower or the higher peaks in the spectrum. This is easily proven by using N-$p_{x,y}$ projected density of states (DOS) calculated for 1 × 1 cells with h-BN in low (N-top, B-fcc) or high (N-fcc, B-hcp) positions, as presented in figure 3(b).

The approach presented here certainly captures the main interactions in the system and, most importantly, explains the essential underlying physics. At the same time it is very competitive in terms of the computational cost compared to a direct *ab initio* calculation. The computational cost to generate the force field is approximately equal to 500 full SCF (self-consistent field) calculations, but only of the small 1 × 1 unit cell. One full SCF calculation of the big nanomesh is approximately 2 × 10^4 more expensive than the calculation of the 1 × 1 unit cell (the most time-consuming parts of the code scale as N^2).

2.2. *Full ab initio calculations*

Although the model calculations presented in the previous paragraph provide an understanding of STM images and UPS spectra, they do not allow us to extract properties that are directly related to the electronic structure of the whole nanomesh unit cell. In order to have access to such properties, but also to verify the force model, we have performed *ab initio* calculations of the whole nanomesh unit cell, containing a 13 × 13 super-cell of h-BN and a 12 × 12 super-cell of the Rh surface. In order to minimize the calculation time of such a huge system, all computational parameters must be chosen with care. By comparing force fields (such as that of figure 1) calculated with different numbers of metal layers, we convinced ourselves that even three metal layers are sufficient for a proper description of the BN–metal interaction. The three metal layers together with two layers of h-BN, placed on both sides of the metal slab (in order to keep inversion symmetry), lead to 1108 atoms in the unit cell. The crucial computational parameter related to the basis set size in the

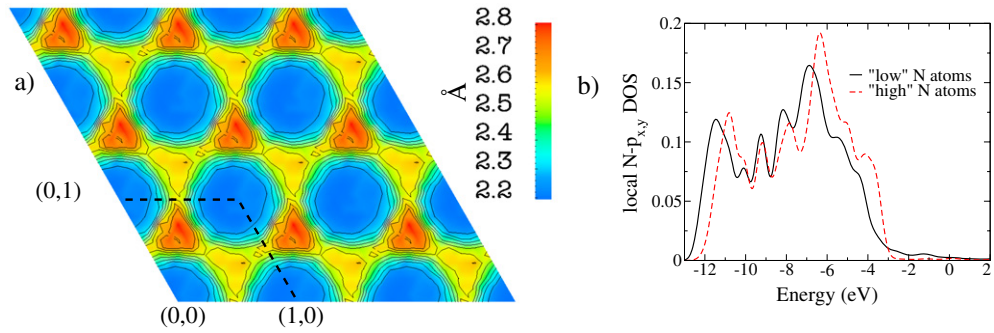

Figure 4. (a) Contour map of the z coordinate of N atoms in the 3 × 3 nanomesh unit cell predicted by *ab initio* calculations. (b) *Ab initio* calculated local density of states projected on N-p$_{x,y}$ state (σ bands) calculated for the 45% highest and 45% lowest N atoms in the full nanomesh unit cell.

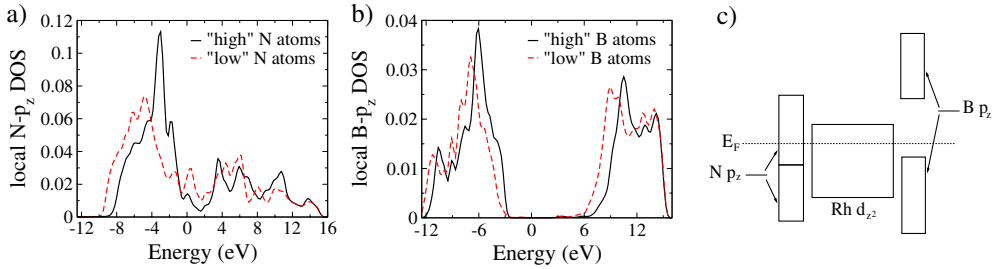

Figure 5. (a) N p$_z$ projected local DOS per atom for the 'low' region and the 'high' region (Fermi level is 0). (b) B p$_z$ projected local DOS. (c) Schematic diagram of the density of states around the Fermi level.

LAPW (linearized augmented plane-wave) method is $RK_{\max}$, which is the product of the smallest muffin-tin sphere radius R times the length of the largest reciprocal vector K of the plane-wave basis. In our case, a $RK_{\max}$ value of 3.3 with sphere radii of B, N and Rh equal to 0.614, 0.783, 1.296 Å, respectively, leads to about 50 000 plane waves and gives converged forces for all atoms. For the exchange–correlation potential the recent Wu–Cohen-generalized gradient approximation (GGA) has been used [21], as it gives, in general, a better description of solids [20] than the more common PBE-GGA [15]. The Brillouin zone was sampled with a single k-point at Γ, which, for sure, delivers good enough accuracy in particular with only three-layer approximation of the metal surface. The optimal z-positions of N atoms presented in figure 4(a) can be compared directly with the results obtained from the force field calculations. As one can see, the separation of the h-BN layer in the two regions, the areas of these regions and the relative heights are very similar. Relaxation of the interface Rh layer, which was neglected in the force model described above, plays a minor role. In a full relaxation we find that the Rh atoms in the interface layer have a corrugation of less than 0.03 Å and the Rh atoms relax outwards (towards BN) when BN is close to (fcc, top), while the underlying Rh relaxes inwards when BN is in the 'high' position. The *ab initio* calculated N-p$_{x,y}$ projected density of states for N atoms that belong either to 45% of the highest or 45% of the lowest positions above the surface are shown in figure 4(b). This result corresponds to the DOS presented in figure 3(b) (from model calculations on the 1 × 1 unit cell), and clearly shows similar features, proving that our previous understanding of the origin of the σ-band splitting was correct. This mainly originates from a larger charge transfer from BN towards Rh when BN is in the 'low' position compared to BN in the nonbonding 'high' position.

The peculiar interaction of h-BN with the Rh(111) surface originates from the hybridization of the N- and B-p$_z$ states with Rh-d$_{z^2}$ states. The force maps (figure 1) show that the combined interaction is always a result of a competition between an attraction of the B atoms and a repulsion of the N atoms. In the 'low' region of the nanomesh the attractive force on B is bigger than the repulsive force acting on N, and therefore h-BN buckles slightly (by about 0.14 Å), with B being closer to the surface than N, until the elastic response of the h-BN layer equilibrates the forces. In this region, h-BN is strongly attracted to the surface. On the other side, in the 'high' region, the repulsive force acting on N atoms exceeds the attraction of B atoms, and the whole h-BN layer bends away from the metal surface. In this position h-BN is repelled from the surface and only the elastic forces originating from the strong sp^2 bonds between B and N acting in the hexagonal plane keeps the layer intact. The calculated partial DOS and the schematic diagrams presented in figure 5 characterize the chemical bonding. As mentioned above, Rh becomes slightly negatively charged by BN. The atomic p-state of the N atom is lower in energy than that of B, and a charge transfer from B to N leads to a negatively charged N. Because of this, the Rh-N interactions are more ionic (repulsive) than covalent and, furthermore, the whole bonding, nonbonding as well as a large part of the antibonding bands are below the Fermi level. For the electropositive B, the situation is different. The corresponding atomic p-state is located at higher energy and a strong covalent

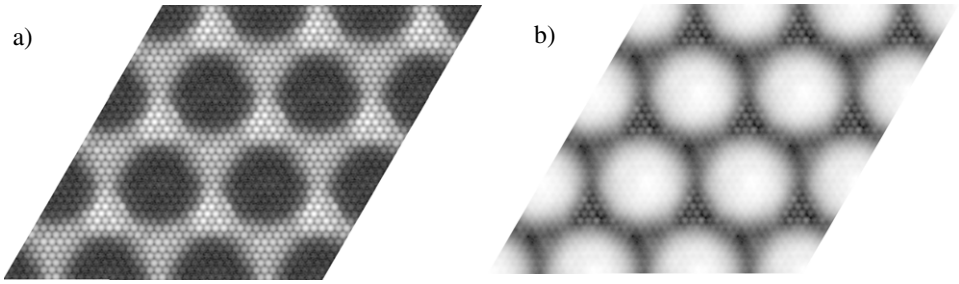

Figure 6. (a) STM images (electron density) calculated from states that are in an energy window of 1 eV centered at 2 eV below the Fermi level. The density is plotted 2 Å above the h-BN 'low' region (b), the same as (a), but the energy window is centered 2.5 eV above the Fermi level and the density is plotted 3 Å above the nanomesh surface. In both cases, low density regions are represented by black and high density regions are represented by white.

interaction between B-p_z and Rh-d_{z^2} leads to a large splitting into bonding and antibonding states. As can be seen from figure 5, all antibonding states are well above the Fermi level and are thus not occupied. This explains why B atoms are attracted to the surface, whereas N atoms are repelled. In the nanomesh unit cell the DOS of the 'high' region gets more weight at higher energies compared to the 'low' region, as seen in figures 5(a) and (b) and already found from simple (1 × 1) model calculations.

Although, the structure of the h-BN layer is certainly compatible with the experimental STM images, for a direct comparison with experiment we need simulated STM images, which are available only from an *ab initio* calculation of the whole unit cell. According to Tersoff and Hamann [19], such images can be obtained from the charge density originating from a set of eigenstates within a certain energy window around E_F corresponding to the applied voltage in the experimental STM measurements. Figure 6 shows such densities produced for an energy window of 1 eV centered on energies 2 eV below (figure 6(a)) and 2.5 eV above the Fermi level (figure 6(b)). The density is displayed in a hexagonal plane located 2 and 3 Å above the h-BN 'low' region for figures 6(a) and (b), respectively. In both cases the 'low' and 'high' regions can be well distinguished. For the scan below the Fermi level, the 'low' regions show lower contrast (smaller local density of states) than the 'high' region. This situation corresponds well to the interpretation of the experimental STM images [2, 5]. However, for the scan above the Fermi level, the contrast seems to be inverted. The 'low' regions show higher local density of states then the 'high' regions. In this case the image corresponds to a contrast observed for h-BN/Pt(111) [18]. In any case, probing states in the vicinity of E_F will always image the N atoms, since the B-p_z local DOS (LDOS) shows a large gap around E_F due to the strong bonding–antibonding interaction with Rh-d_{z^2} states (see figure 5(b)).

3. Concluding remarks

An alternative structural model of the BN nanomesh on the Rh(111) surface consists of a single BN layer with a 12 × 12 Rh and 13 × 13 BN periodicity to accommodate the lattice mismatch. Due to the variation in chemical bonding of BN above different Rh sites, the h-BN monolayer is highly corrugated, which explains the existing STM images as well as the measured splitting of the σ bands. The structure is unique and quite different from common strain relief patterns or dislocation networks, since the lateral BN distances remain almost unchanged throughout the nanomesh. Originally the geometry of the h-BN layer was calculated on the basis of an *ab initio* generated force field. This approach is very effective in terms of computational time and, as we have shown in this contribution, is still quite accurate. In this work we report full *ab initio* calculations of the single layer h-BN/Rh(111). The calculated geometry of the h-BN layer is very similar to the structure predicted by the force field approach, which validates this simple method and our understanding of the interactions in the system. Similarly to the predictions of the force field model, the *ab initio* calculated density of states projected on $p_{x,y}$ of the 'low' and 'high' N atoms shows a 1 eV splitting. The STM images cannot be calculated within the force field approach. However, they are available from the full nanomesh *ab initio* calculations. The presented images agree very well with measured STM images. As expected, 'low' and 'high' regions show, respectively, low density and high density for STM scan probing states below the Fermi level.

Acknowledgments

This work was supported by the European Union (FP6-013817), the Austrian Research Fund (SFB Aurora F1108) and the Austrian Grid Project (WP-A7).

References

[1] Auwärter W, Kreutz T J, Greber T and Osterwalder J 1999 *Surf. Sci.* **429** 229
[2] Berner S, Corso M, Widmer R, Groening O, Laskowski R, Blaha P, Schwarz K, Goriachko A, Over H, Gsell S, Schreck M, Sachdev H, Greber T and Osterwalder J 2007 *Angew. Chem. Int. Edn Engl.* **46** 5115
[3] Blaha P, Schwarz K, Madsen G K H, Kvasnicka D and Luitz J 2001 *WIEN2k, An Augmented Plane Wave Plus Local Orbitals Program for Calculating Crystal Properties* (Austria: Vienna University of Technology)
[4] Bunk O, Corso M, Martoccia D, Herger R, Willmott P R, Patterson B D, Osterwalder J, van der Veen J F and Greber T 2007 *Surf. Sci.* **601** L7
[5] Corso M, Auwärter W, Muntwiler M, Tamai A, Greber T and Osterwalder J 2004 Boron nitride nanomesh *Science* **303** 217

[6] Corso M, Greber T and Osterwalder J 2005 *Surf. Sci.* **577** L78
[7] Goriachko A, He Y, Knapp M and Over H 2007 *Langmuir* **23** 2928
[8] Grad G B, Blaha P, Schwarz K, Auwärter W and Greber T 2003 *Phys. Rev.* B **68** 85404
[9] Huda M N and Kleinman L 2006 *Phys. Rev.* B **74** 75418
[10] Laskowski R, Blaha P, Gallauner T and Schwarz K 2007 *Phys. Rev. Lett.* **98** 106802
[11] Morscher M, Corso M, Greber T and Osterwalder J 2006 *Surf. Sci.* **600** 3280
[12] Nagashima A, Tejima N, Gamou Y, Kawai T and Oshima C 1995 *Phys. Rev. Lett.* **75** 3918
[13] Nagashima A, Tejima N, Gamou Y, Kawai T and Oshima C 1995 *Phys. Rev.* B **51** 4606
[14] NDiaye A T, Bleikamp S, Feibelman P J and Michely T 2006 *Phys. Rev. Lett.* **97** 215501
[15] Perdew J P, Burke K and Ernzerhof M 1996 *Phys. Rev. Lett.* **77** 3865–8
[16] Preobrajenski A B, Vinogradov A S and Mårtensson N 2004 *Phys. Rev.* B **70** 165404
[17] Preobrajenski A B, Vinogradov A S and Mårtensson N 2005 *Surf. Sci.* **582** 21
[18] Preobrajenski A B, Vinogradov A S, Ng M L, Ćavar E E, Westerström R, Mikkelsen A, Lundgren E and Mårtensson N 2007 *Phys. Rev.* B **75** 245412
[19] Tersoff J and Hamann D R 1985 *Phys. Rev.* B **31** 805
[20] Tran F, Laskowski R, Blaha P and Schwarz K 2007 *Phys. Rev.* B **75** 115131
[21] Wu Z and Cohen R E 2006 *Phys. Rev.* B **73** 235116